

Supporting Information for J. Am. Chem. Soc. (Communications) JA020615R

First Disyndiotactic Polymer from a 1,4-Disubstituted Butadiene by Alternate Molecular Stacking in the Crystalline State

Toshihiro Tanaka and Akikazu Matsumoto*

PRESTO, Japan Science and Technology Corporation (JST), and Department of Applied Chemistry, Graduate School of Engineering, Osaka City University, Sugimoto, Sumiyoshi-ku, Osaka 558-8585, Japan

Contents

Polymer Stereochemistry.

Figure S-1. Stereoregular polymer sequences for *trans*-1,4-polymers obtained from symmetric 1,4-disubstituted butadienes.

Figure S-2. Relationship between the crystals packing of monomer molecules with different configurations and stereochemical structure of polymers produced during topochemical polymerization of 1,4-disubstituted butadienes. (a) Translational molecular stacking in the column. (b) Alternate molecular stacking in the column.

Experimental procedures.

Figure S-3. IR spectra of poly(1) and poly(2).

Figure S-4. Powder X-ray diffractions of poly(1) and poly(2).

Figure S-5. ORTEP drawings for the crystals of 1-3 and poly(1).

Polymer Stereochemistry.

There are four types of possible stereoregular structures for each *trans*-1,4-polymer of symmetrical 1,4-disubstituted butadiene. (Figure S-1). The stereochemistry of these polymers is represented by two kinds of relationships as follows, one of which is the relative configuration between the two repeating monomer units: when all the repeating relations are *meso*, the polymer is diisotactic, and when they are *racemo*, it is disyndiotactic. Another relationship is the relative configuration between the vicinal carbon centers, being also represented by the same term, *meso* and *racemo*.

The stereochemical structure of the polymers produced during the topochemical polymerization is considered on the basis of the *EZ*-configuration and the stacking of the monomers. When monomer molecules translationally stack in a column in the crystals, both the (*Z,Z*)- and (*E,E*)-isomers provide an identical polymer, the *meso*-diisotactic polymer, irrespective of the monomer configuration (Figure S-2(a)). Here, the dotted lines tie the carbons, which make a new bond during polymerization. On the other hand, when monomers alternately stack in a column, both the (*Z,Z*)- and (*E,E*)-monomers results in the formation of *racemo*-disyndiotactic polymers (Figure S-2(b)).

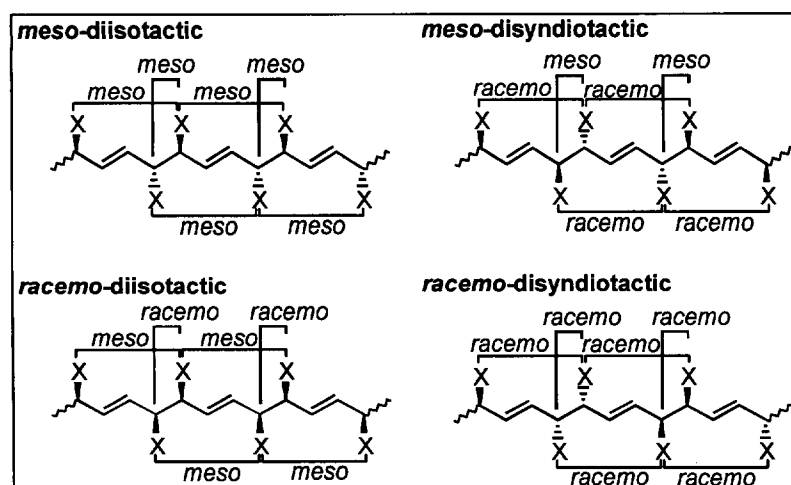


Figure S-1. Stereoregular polymer sequences for *trans*-1,4-polymers obtained from symmetric 1,4-disubstituted butadienes.

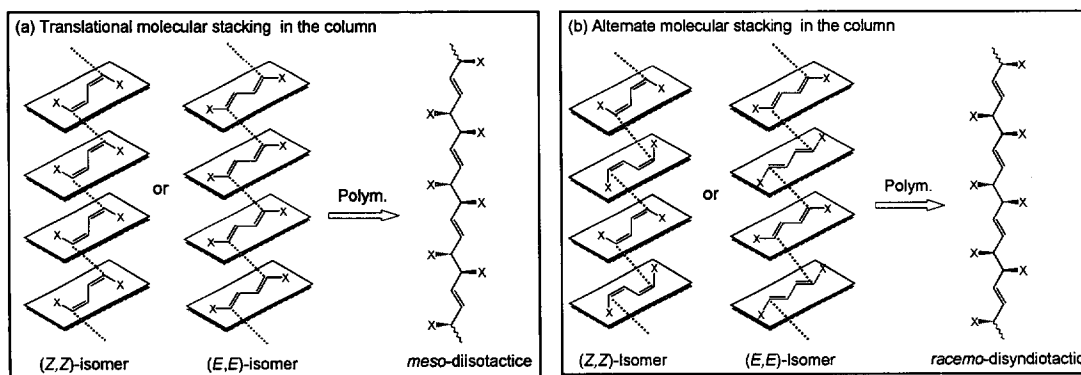


Figure S-2. Relationship between the crystals packing of monomer molecules with different configurations and stereochemical structure of polymers produced during topochemical polymerization of 1,4-disubstituted butadienes. (a) Translational molecular stacking in the column. (b) Alternate molecular stacking in the column.

Experimental procedures.

General Methods. NMR, IR, and UV spectra were recorded on a JEOL JMN A-400, JASCO Herschel FT-IR-430, and JASCO V-550 spectrometer, respectively. The powder X-ray diffraction profile was recorded on RIGAKU RINT-2100 with monochromatized Cu K α radiation ($\lambda = 1.54118 \text{ \AA}$).

Materials. To (Z,Z)-muconic acid (2.08g, 14.5 mmol) in 20 mL of hexamethylphosphoramide in a 100-mL flask equipped with a calcium chloride tube, 4-methoxybenzyl chloride (6.61 g, 42.2 mmol) and potassium carbonate (4.38 g, 31.7 mmol) were added and stirred at room temperature for 3 days. The reaction mixture was poured into 300 mL of saline, and a crude product was extracted with two portions of 150 mL chloroform. After the chloroform solution was washed with water and then dried over sodium sulfate, the chloroform was evaporated under reduced pressure, providing yellowish liquid. To precipitate the 4-methoxybenzyl esters, water and methanol were added to the yellow liquid. The precipitated white solid was filtered and dried under reduced pressure; silica gel column chromatography with chloroform as the eluent provided di(4-methoxybenzyl) (Z,Z)-muconate (**1**) and di(4-methoxybenzyl) (E,Z)-muconate (**3**) as the separate fractions. Yield 3.02 g (54%) for **1**, 0.71 g (24%) for **3**. For the synthesis of di(4-methoxybenzyl) (E,E)-muconate (**2**), the crude product as the mixture of **1** and **3** in chloroform was photoirradiated with a high-pressure mercury lamp at room temperature for 6 h in the presence of small amount of iodide. After evaporation of the chloroform, the isolated yellow liquid was poured into a mixture of water and methanol to precipitate **2** as a white solid. Yield 5.78 g (72%).

Melting point and spectral data for **1-3** are as follows.

For **1**: mp 82.9-83.2°C (CHCl₃); ¹H NMR (400 MHz, CDCl₃) δ 7.91 (m, CH=CHCO₂R, 2H), 7.30-7.35 (m, C₆H₄, 4H), 6.88-6.93 (m, C₆H₄, 4H), 6.00 (m, CH=CHCO₂R, 2H), 5.13 (s, CH₂, 4H), 3.82 (s, CH₃, 4H); ¹³C NMR (100 MHz, CDCl₃) δ 165.48 (C=O), 159.70 (C₆H₄), 138.21 (CH=), 130.18, 127.80, and 124.11 (C₆H₄), 114.00 (CH=), 66.13 (CH₂), 55.30 (CH₃); UV (acetonitrile) λ_{max} 264 nm ($\epsilon = 261000$); IR (KBr) 1584 ($\nu_{\text{C}=\text{C}}$), 1717 ($\nu_{\text{C}=\text{O}}$).

For **2**: mp 119.8-121.8°C (CHCl₃); ¹H NMR (400 MHz, CDCl₃) δ 7.28-7.34 (m, CH=CHCO₂R and C₆H₄, 6H), 6.92-6.88 (m, C₆H₄, 4H), 6.20 (m, CH=CHCO₂R, 2H), 5.14 (s, CH₂, 4H), 3.81 (s, CH₃, 4H); ¹³C NMR (100 MHz, CDCl₃) δ 165.76 (C=O), 159.77 (C₆H₄), 141.08 (CH=), 130.27, 128.31, and 127.70 (C₆H₄), 114.00 (CH=), 65.56 (CH₂), 55.30 (CH₃); UV (acetonitrile) λ_{max} 263 nm ($\epsilon = 28000$); IR (KBr) 1612 ($\nu_{\text{C}=\text{C}}$), 1713 ($\nu_{\text{C}=\text{O}}$).

For **3**: mp 83.8-84.8°C (CHCl₃); ¹H NMR (400 MHz, CDCl₃) δ 8.43 (dd, $J = 15.6 \text{ Hz}$, 11.6 Hz, *trans*-CH=CHCO₂R, 1H), 7.20-7.35 (m, C₆H₄, 4H), 6.87-6.91 (m, C₆H₄, 4H), 6.62 (t, $J = 11.6 \text{ Hz}$, *cis*-CH=CHCO₂R, 1H), 6.11 (d, $J = 15.6 \text{ Hz}$, *trans*-CH=CHCO₂R, 1H), 5.96 (d, $J = 11.6 \text{ Hz}$, *cis*-CH=CHCO₂R, 1H), 5.16 (s, OCH₂, 2H), 5.14 (s, OCH₂, 2H), 3.81 (s, OCH₃, 6H); ¹³C NMR (100 MHz, CDCl₃) δ 165.91 and 165.07 (C=O), 159.67 (C₆H₄), 140.78 and 138.82 (CH=), 130.28, 130.19, 128.97, 127.97, 127.75, and 124.54 (C₆H₄), 114.00 and 113.96 (CH=), 63.34 and 66.26 (CH₂), 55.30 (CH₃); UV (acetonitrile) λ_{max} 266 nm ($\epsilon = 27100$); IR (KBr) 1595 ($\nu_{\text{C}=\text{C}}$), 1711 ($\nu_{\text{C}=\text{O}}$).

Photoreaction. The monomer crystals were photoirradiated with a high-pressure mercury lamp (Toshiba SHL-100-2, 100W, Pyrex filter) at a distance of 10 cm under atmospheric conditions at room temperature. After irradiation, the polymers were isolated by removal of the unreacted monomer with chloroform. The polymer yield was gravimetrically determined. For fabrication of the polymer single crystals of **1**, the monomer single crystals were cut to an appropriate size and charged in a Pyrex tube, degassed, and then sealed. γ -Radiation was carried out with ^{60}Co at room temperature at the Research Institute for Advanced Science and Technology (RIAST), Osaka Prefecture University. The irradiation dose was 200 kGy at a dose rate of 48.6 kGy/h. After irradiation, the quantitative polymer formation was checked by IR spectroscopy and used for the X-ray structure analysis. The authors thank Dr. K. Oka, RIAST, Osaka Prefecture University for providing the γ -radiation facility.

For Poly(**1**): mp 199 °C; IR (KBr) 975 ($\nu_{\text{C}=\text{C}}$), 1735 ($\nu_{\text{C}=\text{O}}$).

X-ray Crystallography. Single crystal X-ray data for **1**, **2** and **3** were collected at $-70\text{ }^{\circ}\text{C}$ and for poly(**1**) at room temperature on a Rigaku R-Axis RAPID Imaging Plate diffractometer using Mo- K_{α} radiation ($\lambda = 0.71073\text{ \AA}$) monochromated by graphite. The structures were solved by a direct method with the programs SIR92 and refined using full-matrix least-squares procedures. All calculations were performed using the CrystalStructure crystallographic software package of the Molecular Structure Corporation.

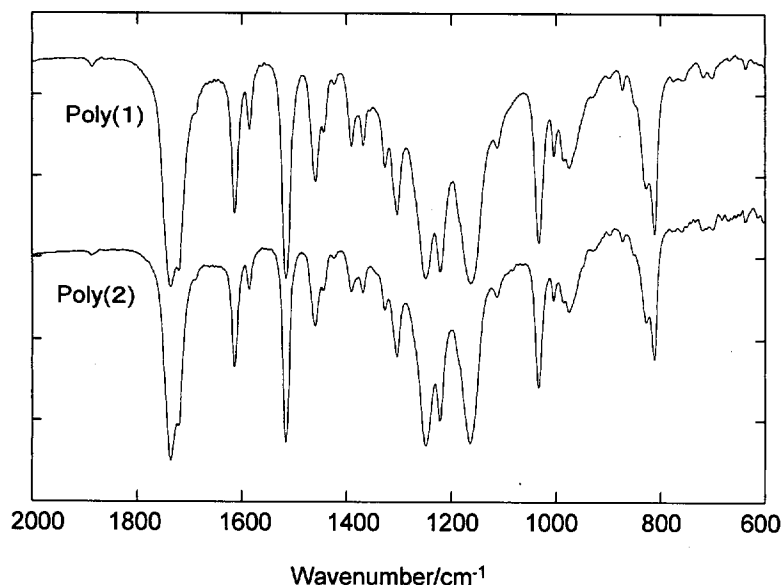


Figure S-3. IR spectra of (a) poly(**1**) and (b) poly(**2**).

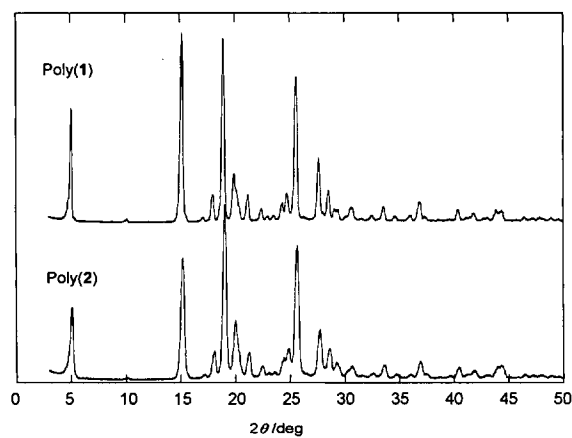
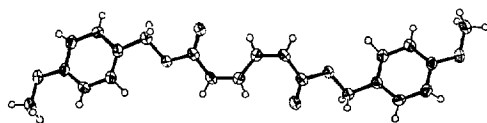
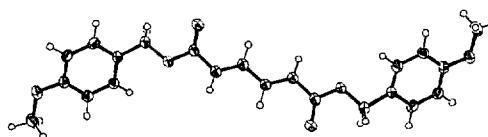


Figure S-4. Powder X-ray diffractions of (a) poly(1) and (b) poly(2).

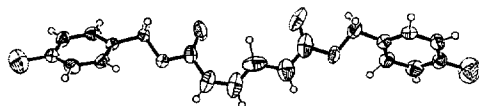
(a)



(b)



(c)



(d)

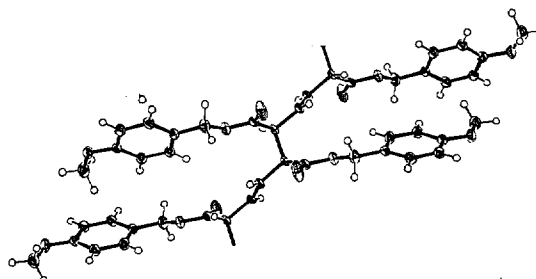


Figure S-5. ORTEP drawings for the crystals of (a) 1, (b) 2, (c) 3, and (d) poly(1).